Electronic Supplementary Material (ESI) for Sustainable Energy & Fuels.

Supporting Information

Correlating oxygen mobility with thermochemical CO_2-splitting efficiency in A-site substituted manganite perovskites

Mahesh Muraleedharan Nair and Stéphane Abanades*

Processes, Materials and Solar Energy Laboratory, PROMES-CNRS (UPR 8521), 7 Rue du Four Solaire, 66120 Font-Romeu, France.

Email: Stephane.Abanades@promes.cnrs.fr

1. Experimental Methods

(i) Material synthesis: Solid-state ceramic process was used for the synthesis of a series of $La_{0.5}A_{0.5}MnO_3$ perovskites used in this study. The perovskite structure can accommodate a large number of cation substitutions in the oxide lattice. The perovskite compositions displaying a favorable trade-off between redox extents and fuel production capacity with minimum stability concerns were chosen for the present study. It is indeed necessary to develop innovative and robust redox materials that can withstand the severe operating conditions of the solar thermochemical process (high-temperature, reducing/oxidizing atmospheres), and that feature high fuel production capabilities at reasonable reaction rates (to maintain the cycling duration as low as possible) with minimum temperature gap between the redox steps (to reduce thermal losses). $SrCO_3$, BaO, CaO, La_2O_3 and MnO_2 were used as cation precursors. In order to eliminate a possible $La(OH)_3$ contamination, La_2O_3 was subjected to a pre-treatment at 950 °C for 6 h under air. Stoichiometric amounts of precursors in accordance with the final $La_{0.5}A_{0.5}MnO_3$ composition, were ground well and calcined at 1000 °C. An additional calcination step depending on the desired phase formation and structure stabilization was carried out at 1500 °C for two hours. The calcination temperature was higher than the reduction temperature used for oxygen release. This is necessary to ensure that structural and phase modifications remain negligible under the reaction conditions. Thermal stability and melting points of the components used in the synthesis were also considered.

The reaction reversibility, oxygen exchange capacity of the materials, thermochemical fuel production yield, and performance stability need to be experimentally investigated, especially in the field of perovskites to identify suitable candidate materials. Alternatively, this work aims to show that considering geometric parameters can be another method to select suitable perovskite compositions for thermochemical redox processes.

(ii) Characterization: Phase identification of the synthesized perovskite oxygen carriers was carried out using X-ray diffraction (XRD) analysis, which is an appropriate and relevant general method to confirm the phase formation and purity of oxides, including perovskites. Diffraction patterns in the wide-angle region (2θ = 20-80 °) were obtained for all the materials using a Philips PW 1820 diffractometer equipped with a Cu Kα radiation (0.15418 nm). Formation of appropriate phase was confirmed by comparing with standard diffraction profiles (PDF-2, International Center for Diffraction Data, ICDD).

(iii) O_2 and CO release via two-step CO_2 splitting experiments: Thermochemical redox experiments were performed via thermogravimetric analysis (TGA) using a SETARAM SETSYS Evolution device (0.03 µg resolution) equipped with a platinum crucible. Blank run correction (using empty crucible) was done to eliminate the small baseline drift during non-isothermal heating caused by thermal gas expansion and buoyancy effects on the crucible. Sample masses of approximately 100 mg were used for each analysis. Thermal reduction step was performed under an Ar flow of 0.020 Nl.min^{-1} (99.999% purity, <2 ppm O_2) at a fixed temperature of 1400 °C during 45 min of temperature plateau. Re-oxidation under CO_2 (50% in Ar) was performed at 1050 °C for 45 min. All heating and cooling steps were performed with a ramp rate of 20 °C.min^{-1}. The O_2 release during reduction induced a mass loss (Δm_{red}) and was used to determine the mole amounts of n_{O2} released during thermal reduction ($n_{O2} = \Delta m_{red}/M_{O2}$). Similarly, the number of moles of CO produced was determined from the mass gain during re-oxidation ($n_{CO} = \Delta m_{ox}/M_O$).

The operating conditions chosen for each cycle were identical for all the considered materials. Thus, comparison of materials performance for identical conditions was possible. Different conditions (higher temperature, CO_2 mole fraction, gas flow rates, reaction durations) may have resulted in higher reaction extents and production rates, but for comparing the materials redox activity, typical conditions and a reasonable cycling time were chosen to perform cycles with a suitable duration for practical implementation in solar thermochemical application. TGA is the most suitable method to monitor accurately the solid-gas reactions (O_2-releasing reduction step inducing sample mass loss and CO_2-splitting step inducing sample mass gain). Furthermore, the method measures directly the reaction kinetic rates from the mass variations, without any induced delay due to the gas detection in outlet gas analyzers. The sample mass variation is directly related to the oxygen exchange capacity. This method thus gives a more definite value of the level of reduction/re-oxidation achieved when compared with gas phase analysis methods, as it eliminates the calibration uncertainty of any gas analysis system. In addition, the TGA is continuous and is able to capture transients and fast changes in reduction extent. TGA data also show whether the samples are returning to the same mass after each cycle.

The CO concentration in outlet gas resulting from TGA does not reflect the real concentration in a large-scale solar reactor. On one hand, in a material-related study performed in a TGA system, the concentration of produced CO is not representative of a real process, given that the amount of solid in the crucible is extremely low (a few mg) compared to the flow of CO_2 to be converted (most of the CO_2 in the stream is not in contact with the crucible and thus directly flows outside). On the other hand, the CO concentration will surely depend on the amount of solid reacting inside the reactor; the higher the amount of loaded active solid, the higher the CO concentration will be. Therefore, direct measurement of mass variations during reduction/re-oxidation studies conducted in a TGA is considered more meaningful for thermochemical redox performance assessment, whereas measuring the CO concentration (or CO/CO_2 ratio) is more relevant for reactor-related studies at a higher scale.

The precision and reproducibility of TGA runs are far beyond the ones required for the study given the high resolution of the apparatus (0.03 µg) whatever the mass analysed, while the minimum mass variation observed for such perovskite-based materials is about Δm = 0.2% (corresponding to about 200 µg given that the sample mass is around 100 mg in the crucible). The balance (fitted with a beam articulated on a torsion ribbon) displays high stability and sensitivity (with a typical mass drift of only 0.1 $\mu g.h^{-1}$) thanks to a high-performance, optical and electronic detection fitting. Based on the stability of the balance, the intrinsic uncertainty could be considered minor when compared with the reduction capabilities and the mass variation of the samples. The uncertainty on the mass change remains below 1 µg, thus representing an uncertainty on the gas productions of ± 0.5 $\mu mol.g^{-1}$. The CO production per unit mass of oxide ($\mu mol.g^{-1}$) is commonly used as a relevant metric for evaluating solar thermochemical CO_2 splitting. It can indeed indicate the fuel production capacity for a given amount of material loaded in a solar reactor. The amount of CO produced depends mainly on the amount of reactive solid, not on the amount of CO_2 fed (this differs from a catalytic reaction). This is thus a main relevant metric to be reported because in a solar process (the targeted application for such materials), the most important outcome will be the fuel production related to the amount of solid oxide loaded in the reactor. Of course, this CO production per unit mass is dependent on the reduction extent (δ) reached during the reduction step, and on operating parameters such as CO_2 flow rate, mole fraction, reaction duration, or temperature. Changing one parameter can modify the CO production rate and yield for a same perovskite material. For instance, the CO_2 flow rate, among other parameters, can affect the performance of the material. Indeed, the thermodynamic barrier can be counteracted by using large oxidant excess (low $CO:CO_2$ ratio) to shift the reaction equilibrium favouring fuel production. In addition, increasing the CO_2 mole fraction also enhances the oxidation kinetic rate. Thus, the conditions were fixed for all the materials to facilitate their performance comparison. Providing fuel production yields in mol/g is thus a suitable way to compare materials performance in this case. In addition to this metric, the reduction and re-oxidation rates ($\mu mol.s^{-1}.g^{-1}$) were also used to compare the thermochemical performance of materials (in Figs. 3 and 4 of the manuscript).

2. Supplementary Figures

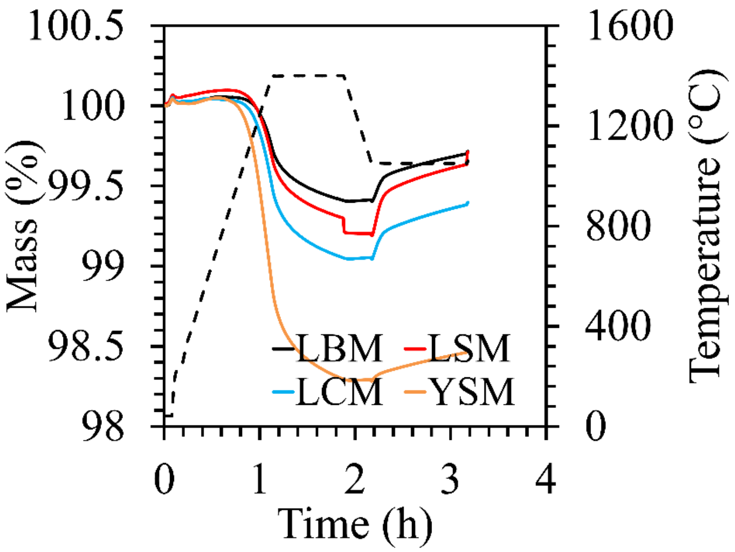

Fig. S1 Mass evolution profiles during reduction and re-oxidation, obtained by performing thermogravimetric analysis for A-site substituted perovskite oxygen carriers. Thermochemical reduction was carried out at 1400 °C and CO_2 induced re-oxidation was conducted at 1050 °C after a cooling step at 20 $°C.min^{-1}$ in Ar (from 1400 to 1050 °C).

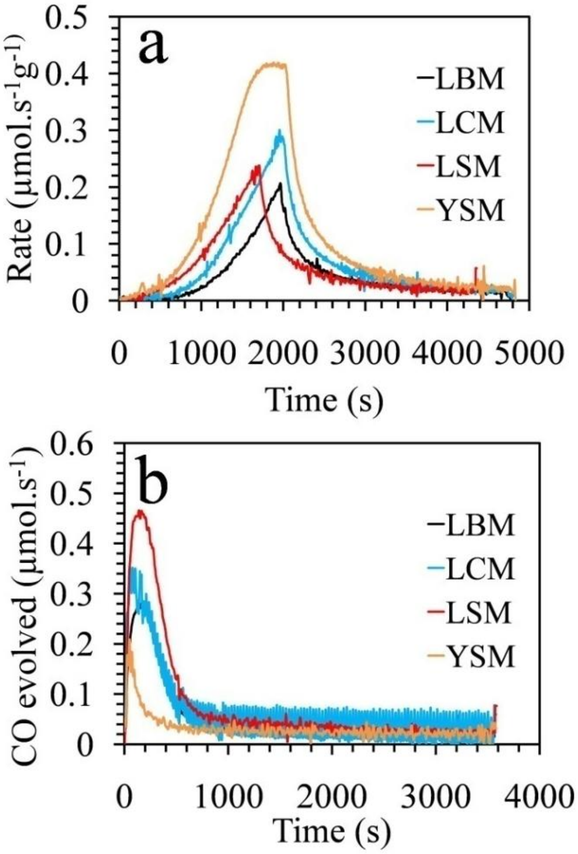

Fig. S2 Reaction rates for O_2 (a) and CO (b) evolution for A-site substituted perovskite oxygen carriers. O_2 release experiments were conducted at 1400 °C and CO release experiments were conducted at 1050 °C.

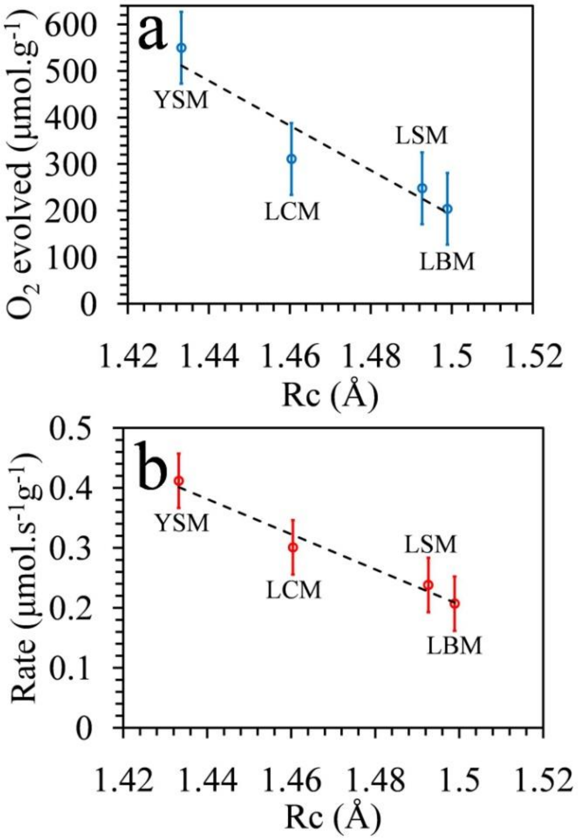

Fig. S3 Evolution of O_2 (a) and reduction rate (b) as a function of critical radius for A-site substituted perovskite oxygen carriers.

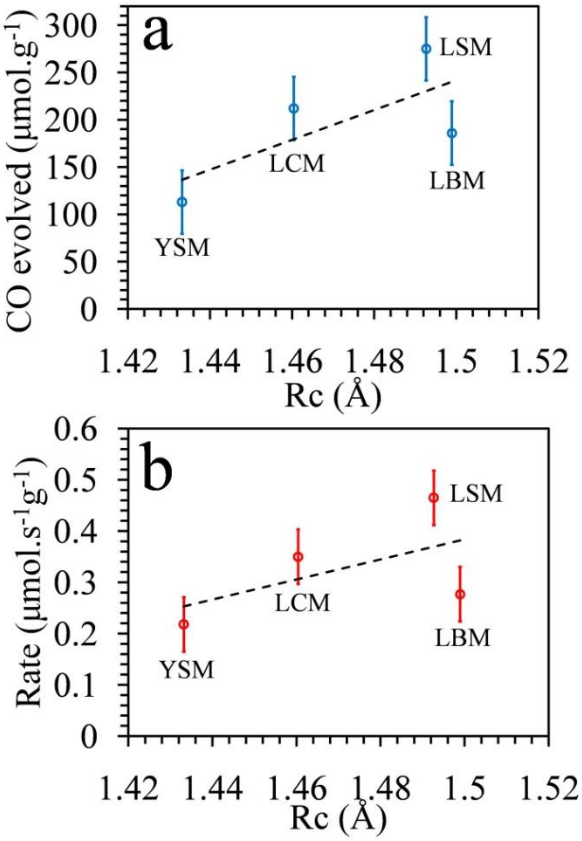

Fig. S4 Evolution of CO (a) and re-oxidation rate (b) as a function of critical radius for A-site substituted perovskite oxygen carriers.

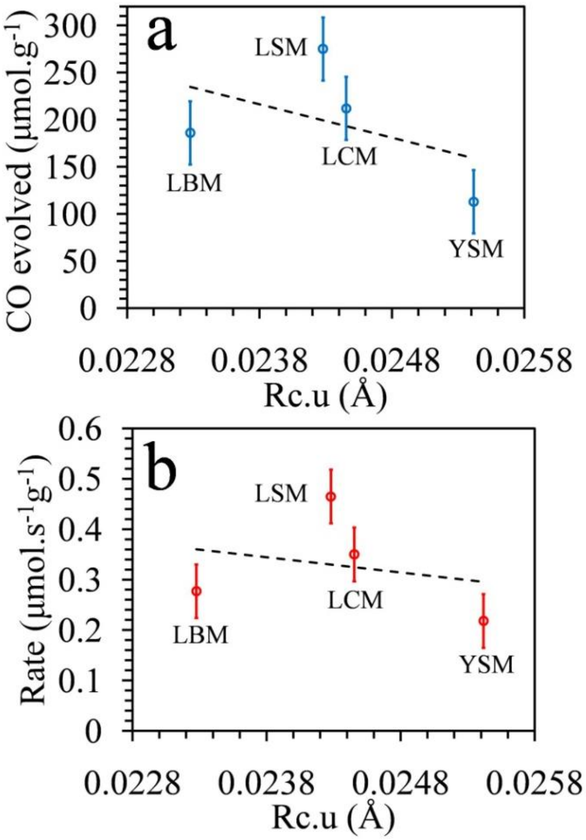

Fig. S5 Evolution of CO (a) and re-oxidation rate (b) as a function of critical radius per unit cell volume for A-site substituted perovskite oxygen carriers.

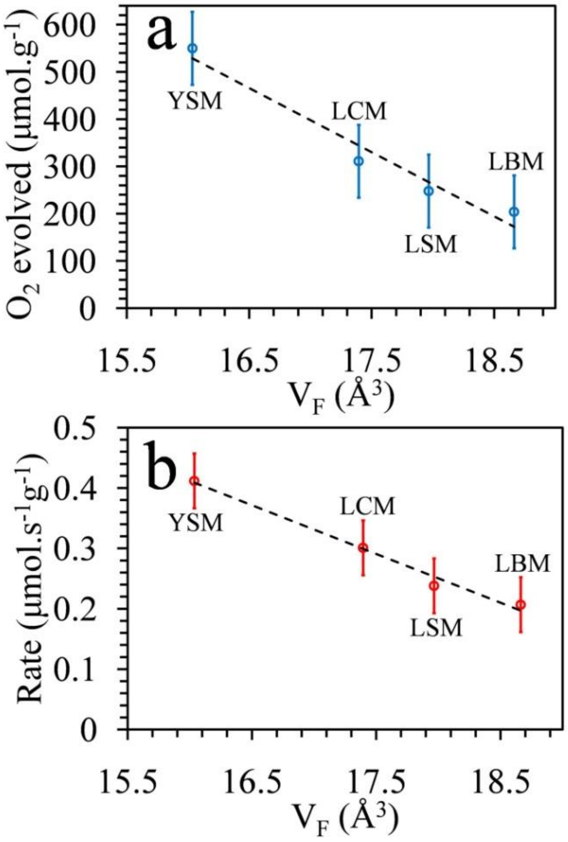

Fig. S6 Evolution of O_2 (a) and reduction rate (b) as a function of lattice free volume for A-site substituted perovskite oxygen carriers.

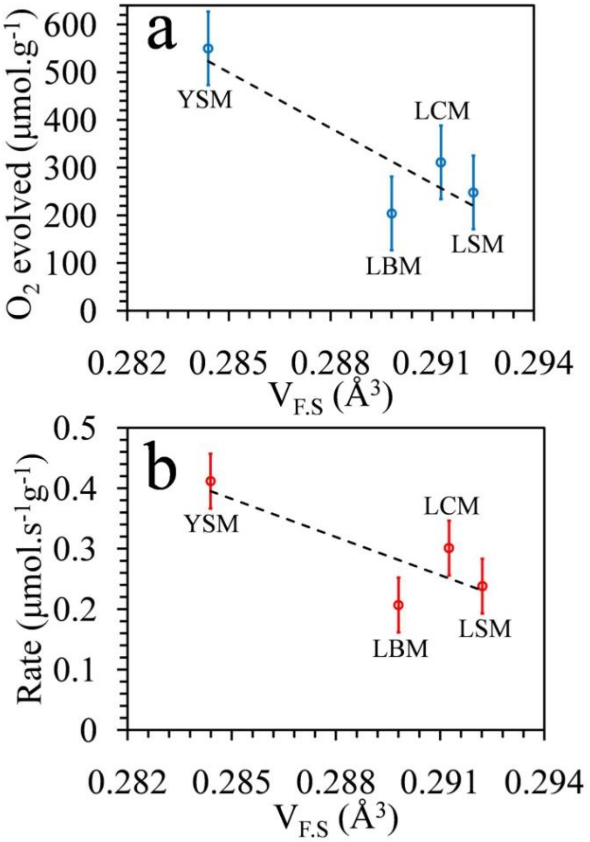

Fig. S7 Evolution of O_2 (a) and reduction rate (b) as a function of specific free volume for A-site substituted perovskite oxygen carriers.

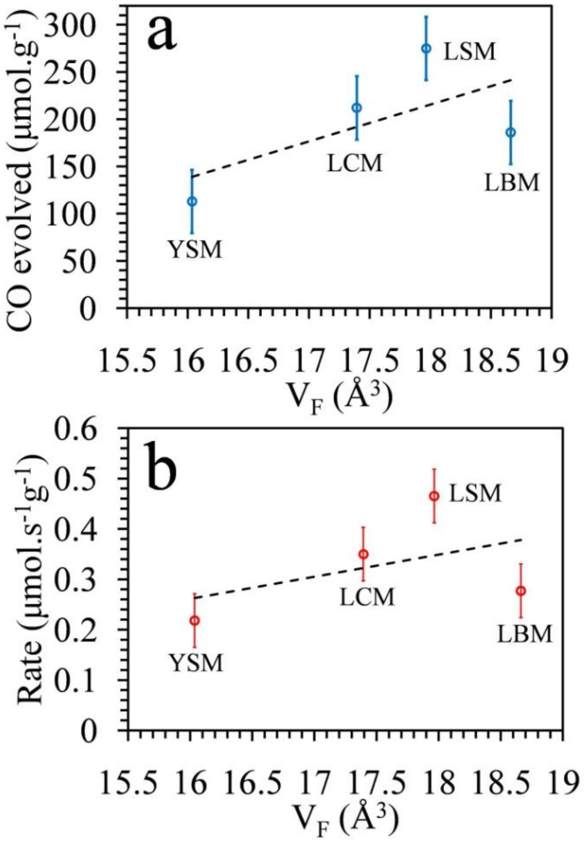

Fig. S8 Evolution of CO (a) and re-oxidation rate (b) as a function of lattice free volume for A-site substituted perovskite oxygen carriers.

3. Supplementary Table

Table S1. Description of the materials used along with their redox activity (including amounts of O_2 and CO evolved and maximum reduction and re-oxidation rates) during thermochemical redox experiments.

Material	**Crystallite size (nm)**	**O_2 evolved (μmol.g^{-1})**	**Maximum rate of reduction (μmol.g^{-1}.s^{-1})**	**CO evolved (μmol.g^{-1})**	**Maximum rate of re-oxidation (μmol.g^{-1}.s^{-1})**
$La_{0.5}Ba_{0.5}MnO_3$ (LBM)	48.09	204	0.207	186	0.350
$La_{0.5}Ca_{0.5}MnO_3$ (LCM)	45.55	311	0.301	212	0.277
$La_{0.5}Sr_{0.5}MnO_3$ (LSM)	47.53	248	0.238	275	0.465
$Y_{0.5}Sr_{0.5}MnO_3$ (YSM)	39.47	550	0.412	113	0.218